VILNIUS TECH
Vilnius Gediminas Technical University

AVIATION
ISSN: 1648-7788 / eISSN: 1822-4180
2022 Volume 26 Issue 1: 64–71
https://doi.org/10.3846/aviation.2022.15963

INDICATED AIRSPEED ERROR DUE TO GRADUAL BLOCKING OF PITOT TUBE WITH DRAIN HOLE

Filip SKLENÁŘ *, Jiří MATĚJŮ

Institute of Aerospace Engineering, Faculty of Mechanical Engineering, Brno University of Technology, Czech Republic

Received 20 October 2020; accepted 8 May 2021

Abstract. Problem of pitot tube blocking is persistent because even in the recent past there have been several accidents based on inaccurate information from air speed indicators. This problem was caused by a partial or complete blockage of the total pressure probes. Certain principles of blocking detection are well known. This article describes research into another principle of the gradual blocking detection of the pitot tube with drain holes. Pitot tubes with different blockage ratios were made and tested. A gradual blocking curve was described. The independence of velocity magnitude for the investigated airspeeds was found. This research shows that the drain hole design can be useful for a pitot tube blockage detection. The principle is based on another pitot tube with a larger drain hole area. Airspeed error due to gradual blocking grows faster on the other pitot tube. Gradual blocking of both pitot tubes results in a difference in indicated airspeeds, even at constant speed flight and before full blockage. This airspeed difference can warn a pilot and gives him or her a valuable time to use emergency procedures.

Keywords: pitot tube, total pressure, static pressure, blocking, unreliable airspeed.

Introduction

At the beginning, there was a hypothesis about the dependence of the total pressure measurement on the pitot tube inlet. The first wind tunnel test of a blockage of the LUN 1150 pitot tube (manufactured by Microtechna a.s.) showed a gradual change of the indicated airspeed with the total pressure inlet blockage. It was found that the gradual change of the indicated airspeed is caused by the drain hole on the pitot tube. If the pitot system is ideally pressure-tight, the total pressure is independent of the inlet area (see section 2.1). However, the majority of pitot tubes, generally used in aircraft, have drain holes. The drain holes are important to tackle problems with humidity in practical flight operations. On the other hand, they cause the pitot-static system not to be pressure tight. It is a leakage outlet. This research studies the effect of drain holes and discuss a principle of blocking detection based on this effect.

The basic instruments that a pilot uses to control an aircraft indicate air data parameters. These include an airspeed indicator, altimeter, and vertical speed indicator (Federal Aviation Administration (FAA), 2016). The air speed indicator is one of the most important parameters for flight safety. Calibrated airspeed (CAS) is crucial information for pilots in terms of flight envelope regime identification. It is necessary to maintain the airspeed within certain limits. If the aircraft flies too slowly, there is a risk of stall or spin (EASA, 2013). If the aircraft exceeds an allowed speed limit, a risk of structural failure exists. The pitot static system is the most frequently used way of obtaining airspeed, because it is convenient to compute the airspeed from dynamic pressure. Airspeed measurement by a pitot-static system is influenced by the instrument error, position error, manoeuvrability error, density error and compressibility error (Oxford Aviation Academy, 2008). These errors can be corrected by well-known procedures. The problem is where an error arises which is caused by degradation or failure of the system, e.g., a pitot tube which is blocked by a cover, insects, icing and so on. This has caused a lot of emergency situations and accidents in the past (e. g., AAIB Bulletin 11/2020, 2020; Australian Transport Safety Bureau, 2018; Bureau d'enquêtes et d'analyses pour la sécurité de l'aviation civile, 2012; Flight Safety Foundation, 1995; The Interstate Aviation Committee, 2018; Japan Transport Safety Board, 2018; National Transportation Safety Board, 2013).

Several solutions to a safe flight with malfunctioning airspeed indicator have been developed in the past if the

*Corresponding author. E-mail: *filip.sklenar@vutbr.cz*

problem with a pitot static system is detected. A system and method for calculating the Mach number and True Airspeed (TAS) without information from the pitot static system was patented (Nathan & Anandappan, 2014). Mach number and TAS are calculated from altitude information from GPS, an inertial navigation system, a radio altimeter, and other sensors on board without the use of an Air Data Computer. Similar research analyses the possibility of detecting faults in the pitot tube of Unmanned Aerial Vehicle (UAV) (Hansen et al., 2010). Still other research focuses on developing a method for detecting UAV sensor faults by using existing sensors (Guo et al., 2018). Further research describes robust fault detection for commercial transport air data probes (Freeman et al., 2011). However, these methods can only be used in large aircraft or UAV with modern electronic equipment. A partial solution for smaller aircraft was developed by the Aspen Company (Genito et al., 2018). Their system displays Angle of Attack (AoA) on the Primary Flight Display PFD or Multifunction Flight Display MFD. The AoA information is calculated from the flight envelope data received from the air data computer and attitude heading reference system AHRS and certified GPS. The AoA is an essential parameter for flight. It may show a risk of stall or spin, but it is not indicative of the risk of exceeding the maximum speed. The system does not inform the pilot in the event of a malfunction of air speed measurement.

During the take-off phase, pilots can recognize pitot-static system blockage by checking if the airspeed indicator moves ("airspeed alive" check) (Parker, 2007). A slow gradual blockage during the flight is dangerous, because it is difficult for a pilot to recognise it (Federal Aviation Administration, 2016). A gradual blockage of the pitot tube during flight is usually caused by growing ice on the pitot tube in freezing conditions. The "speed alive check" does not work in this situation as the speed is usually kept constant. Therefore, detecting the gradual blockage of the total pressure inlet at constant speed can be essential information for a pilot.

The principle described in this study gives an alternative to existing systems. The ice blocking mechanisms were studied also by Lv et al. (2020). They studied the semi-quantitative law of rime ice, glaze ice, water spray and non-ice organic material blocking mechanisms. In the studied cases, no blockage of static ports was observed; only total ports were blocked. They suggested that the second pitot tube system in the different position on the aircraft was just for ice detection. The system does not take into account the useful effect of the defined leakage (for example, drain holes) described in this paper. In the past, other icing detection systems were developed, e.g., a pitot tube with integrated sensors that measures temperature, thermal conductivity and impedance (Jarvinen, 2011). Another system was designed for detection and warning of ice crystals clogging pitot probes from total air temperature anomalies (Ayra et al., 2020). These systems are able to detect only icing, but unable to detect another blockage. The use of phase change materials was tested (Jäckel et al., 2020). This solution can slow down the cooling of the pitot tube in the case of a heating element failure. However, it cannot prevent icing. A system that is able to detect almost all types of blockage uses fiber optic sensors combined with actuators to monitor and maintain pitot tube correct operation under different environmental conditions (Jackson, 2015). This system could detect blockages by ice, volcanic ash, sand and insects. The system is based on a different physical principle in comparison to this research and requires a special electronic device. A system of detection of failure of the aerometric system on Unmanned Aerial System (UAS) is presented also by Sun and Gebre Egziabher (2020). The detection is based on two separate pitot-static tubes, the data from which is corrected by data from Inertial Measurement Unit (IMU). This system does not take into account the defined leakage effect presented in this study.

In this paper another principle of detecting the pitot tube blockage based on drain hole effect is suggested. A drain hole effect is experimentally measured for various velocities and various inlet and drain holes area. The change of indicated airspeed with blockage of the total pressure inlet is examined. The gradual blocking curve is described. Inflight blocking scenarios of the pitot tube are discussed with respect to the suggested principle of blocking detection.

1. Methodology

In this study, the throttling in the inlet of pitot tube was simulated by inlet diameter change. The gradual blocking is highly dependent on the inlet area to drain hole area ratio A_inlet/A_drain. It gives us very good insight to the problematic. Ten pitot tubes were manufactured with various inlet diameters (see Table 1, Figure 1). The diameter of the pitot tubes was 10 mm and the length was 95 mm (see Figure 2). The drain holes were placed 35 mm behind the inlet.

Four drain holes were drilled into the side of each tube. Two holes with the diameter of 0.5 mm and two more with a diameter of 1 mm. The drain holes were opened and closed according to the required drainage area. Pitot tubes were tested in a low-speed closed circuit wind tunnel with 500 × 700 × 2000 mm closed test section where the undisturbed flow turbulence intensity is lower than 0.3%.

Table 1. Pitot tube hole diameters

Pitot tube number	Total pressure inlet diameter (mm)	Pitot tube number	Total pressure inlet diameter (mm)
1	0.2	6	1.2
2	0.3	7	1.6
3	0.5	8	2.0
4	0.8	9	2.5
5	1.0	10	3.0

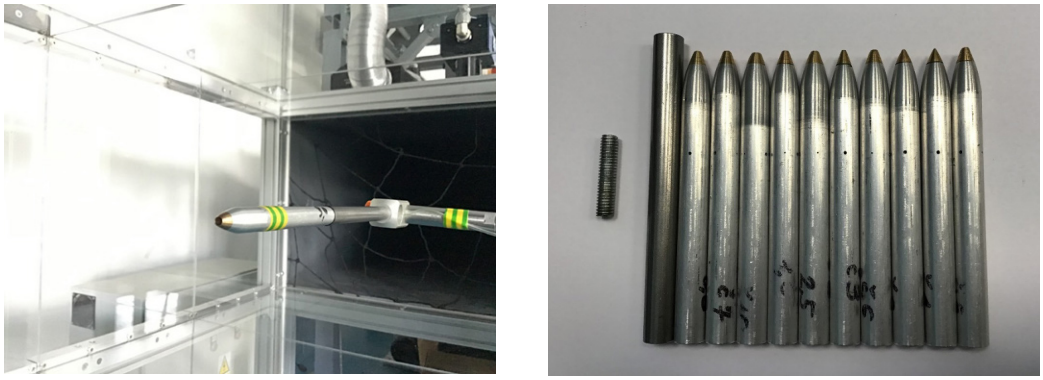

Figure 1. Pitot tube wind tunnel installation (left) and ten pitot tubes with various inlet diameters (right)

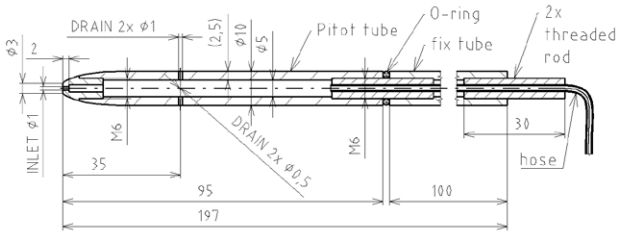

Figure 2. Dimensions of the pitot tube with drain holes

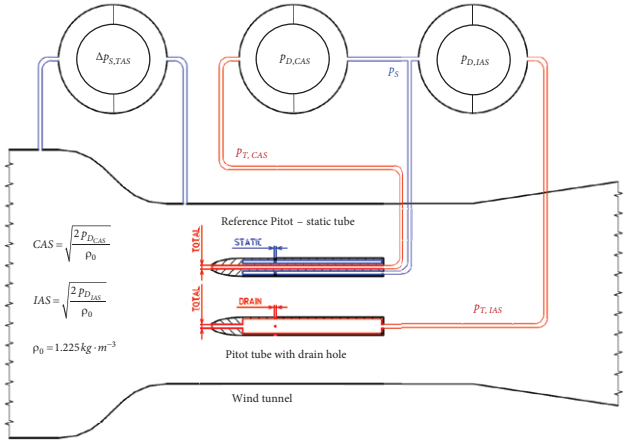

Figure 3. The wind tunnel test section with probes and pressure sensors connection (scheme not to scale: pitot static tube diameter is 4 mm, the drain hole pitot tube diameter is 10 mm and the test section is 500 × 700 × 2000 mm. The wind tunnel blockage ratio is 0.02%)

In the wind tunnel, TAS was adjusted to the inlet. TAS was computed by the inner wind tunnel procedure from differential pressure sensor ($\Delta p_{S_{TAS}}$) and other temperature and pressure sensors on the diffusor part of the tunnel. Dynamic pressure $p_{D,CAS}$ was measured on the reference pitot static tube. Dynamic pressure $p_{D_{IAS}}$ was measured on the examined pitot tube with drain hole (see Figure 2). Static pressure was taken from reference pitot static tube to both dynamic pressure sensors. Airspeed was computed using the equations listed in Figure 3, where TAS is the airspeed adjusted on the wind tunnel control panel, CAS is the airspeed detected on the reference pitot static tube, and Indicated Airspeed (IAS) is the airspeed detected on the pitot tube under test with various inlet and drain holes areas. The tests were performed for four true airspeeds commonly occurring in general aviation (25 $m \cdot s^{-1}$ – take off speed, 35 $m \cdot s^{-1}$ – initial climb speed, 50 $m \cdot s^{-1}$ – economic cruise speed and 60 $m \cdot s^{-1}$ – cruise speed). Atmospheric pressure during the experiment was 98330 Pa and air temperature 23 °C. The exact conditions slightly changed with every measured case. A total of 168 cases were measured. Ten samples were recorded for every case. The data was transformed to indicate airspeed which refers to the international standard atmosphere and allows comparison.

2. Results of experiments

2.1. Dependency of IAS on inlet area with drain holes closed and conditions of the experiment

Experiments 1, 2, 41 and 42 tested an inlet diameter of 0.2 and 3 mm with all drain holes closed. The deviation of the indicated airspeeds from the calibrated airspeed was within ±0.3 $m \cdot s^{-1}$ interval for both inlet diameters at all tested airspeeds. It proved no dependency of the indicated airspeed on inlet diameter with drain holes closed.

2.2. Dependency of IAS on inlet area with drain hole opened

This section describes the change of IAS due to a change of the pitot inlet hole area A_{inlet} with the fixed drain hole area A_{drain}. The dependency is described by the gradual blocking curve. The gradual blocking curve shows the IAS / CAS ratio dependence on the A_{inlet} / A_{drain} ratio. Examined variables in the experimental setup with the drain hole opened is provided in a shortened list of setups in the table below. Parameter A_{drain} represents the sum of all the drain hole areas opened. Experiment setups 3 to 12 were done with one drain hole with 1 mm diameter opened (see Table 2).

Figure 4 shows the dependency of IAS on the inlet area for a 1 mm drain hole diameter (A_{drain} = 0.8 mm^2). The lines with the same colour refer to the constant CAS. IAS (circle symbols lines) were computed from dynamic pressure on the pitot tube with the drain holes. CAS (cross

Table 2. Experiments with 1 mm drain hole opened and 25, 35, 50 and 60 m/s TAS

Exp. No.	Pitot No.	D_{inlet} [mm]	$\frac{A_{inlet}}{A_{drain}}$	Inlet area to drain area ratio	$D_{drain,\ 3}$ [mm]
3	10	3	9.0	9.0 × larger inlet area to drain area	1
4 to 11	9 to 2	…	…	…	1
12	1	0.2	0.04	25.0 × lower inlet area to drain area	1

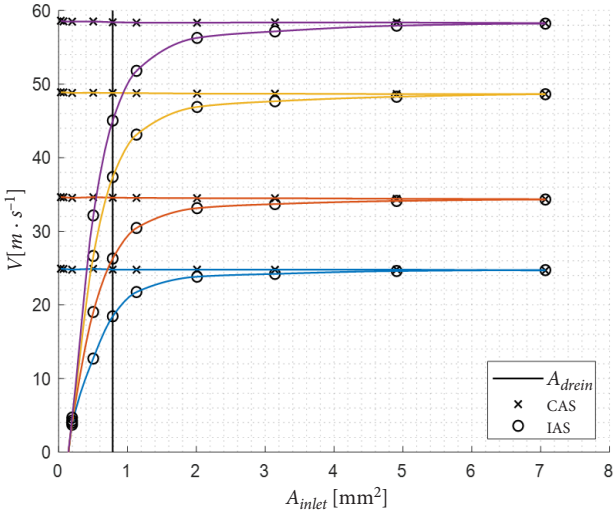

Figure 4. Indicated airspeed IAS on the inlet area for a pitot tube with 1 mm drain hole diameter

symbols lines) were computed from dynamic pressure on the reference pitot tube. At constant CAS, a gradual decrease in IAS was found with the decrease of the inlet area. The IAS decreased slowly if $A_{inlet} > A_{drein}$. A rapid decrease in IAS at given CAS is evident if the inlet area is lower than drain hole area ($A_{inlet} < A_{drein}$).

Figure 5 shows the dependence of IAS / CAS ratio on the A_{inlet} / A_{drain} ratio with A_{drain} = 0.79 mm^2. This dependency is called "a gradual blocking curve" in this study. The gradual blocking curve is independent of CAS for tested speeds from 25 $m \cdot s^{-1}$ to 60 $m \cdot s^{-1}$. This means that the decrease in IAS in the percentage of CAS, due to increasing blockage, is independent of the airspeed.

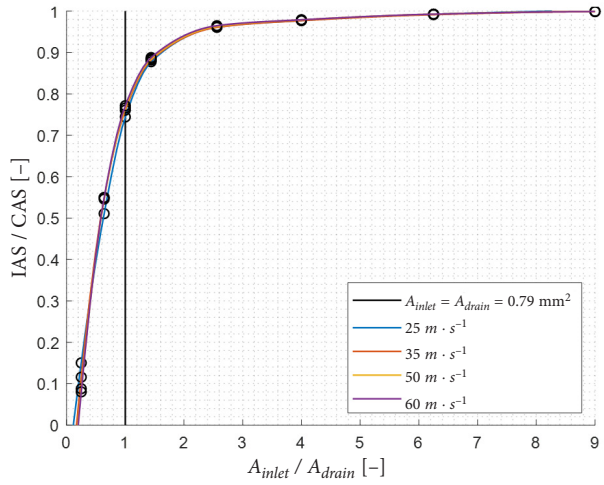

Figure 5. Gradual blocking curve *IAS / CAS* ratio A_{inlet} / A_{drain} ratio for a pitot tube with 1 mm drain hole diameter

2.3. Dependency of IAS for varying inlet and drain hole area

This section shows the gradual blocking curve for changing inlet and drain hole area. It shows a higher range of A_{inlet} / A_{drain} ratio. A shortened list of experiment setups with drain holes opened is provided in the tables below (see Table 3, Table 4). Experiment setups 13 to 22 were tested with one drain hole with a 0.5 mm diameter opened.

Experiment setups 23 to 32 were tested with 1 drain hole with 0.5 mm and two with 1 mm diameter opened.

Experiment setups 33 to 40 were tested with various combinations of inlet and drain holes (see Table 5). It helped to describe the maximum range of the A_{inlet} / A_{drain} ratio.

Table 3. Experiments with a 0.5 mm drain hole opened and 25, 35, 50 and 60 m/s TAS

Exp. No.	Pitot No.	D_{total} [mm]	$\frac{A_{inlet}}{A_{drain}}$	Inlet area to drain area ratio	$D_{drain,\ 1}$ [mm]
13	10	3	36.0	36.0 × larger inlet area	0.5
14 to 21	9 to 2	…	…	…	0.5
22	1	0.2	0.16	6.3 × lower inlet area	0.5

Table 4. Experiments with one 0.5 mm drain hole and two 1 mm drain holes opened 25, 35, 50 and 60 m/s

Exp. No.	Pitot No.	D_{total} [mm]	$\frac{A_{inlet}}{A_{drain}}$	Inlet area to drain area ratio	$D_{drain,\ 1}$ [mm]	$D_{drain,\ 2}$ [mm]	$D_{drain,\ 3}$ [mm]	$D_{drain,\ 4}$ [mm]
23	10	3	4.0	4.0 × larger inlet area	0.5	closed	1	1
24 to 31	9 to 2	…	…	…	0.5	closed	1	1
32	1	0.2	0.02	56.3 × lower inlet area	0.5	closed	1	1

Table 5. Experiments with maximum range of A_{total} to A_{drein} ratio

Exp. No.	Pitot No.	D_{total} [mm]	$\frac{A_{inlet}}{A_{drain}}$	Inlet area to drain area ratio	$D_{drain,1}$ [mm]	$D_{drain,2}$ [mm]	$D_{drain,3}$ [mm]	$D_{drain,4}$ [mm]
33	9	2.5	25.0	25.0 × larger inlet area	0.5	closed	closed	closed
34	8	2	8.0	8.0 × larger inlet area	0.5	0.5	closed	closed
35	7	1.6	2.6	2.6 × larger inlet area	closed	closed	1	closed
36	6	1.2	1.15	1.15 × larger inlet area	0.5	closed	1	closed
37	5	1	0.44	1.5 × lower inlet area	0.5	0.5	1	closed
38	4	0.8	0.32	3.1 × lower inlet area	closed	closed	1	1
39	3	0.5	0.11	9.0 × lower inlet area	0.5	closed	1	1
40	2	0.3	0.04	27.8 × lower inlet area	0.5	0.5	1	1

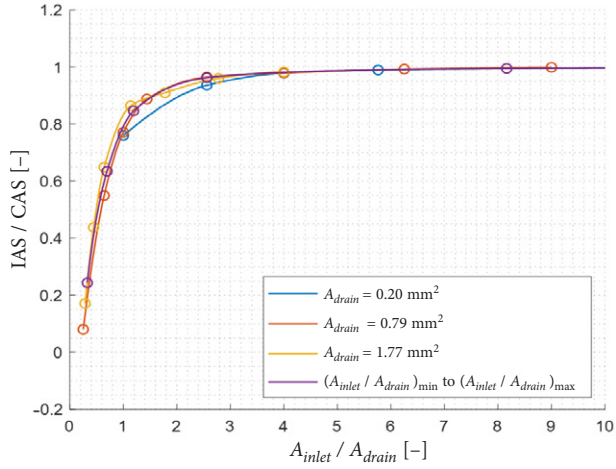

Figure 6. Gradual blocking curve *IAS / CAS* ratio on A_{inlet} / A_{drain} ratio for pitot tube at 60 $m \cdot s^{-1}$ for various drain hole areas

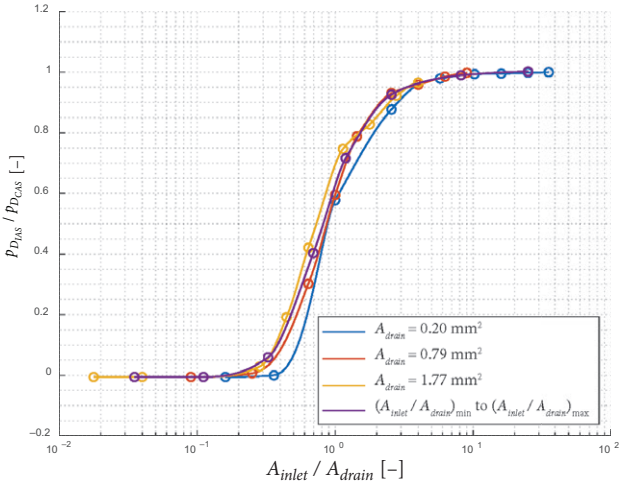

Figure 7. Gradual blocking curve $p_{D_{IAS}}$ / $p_{D_{CAS}}$ ratio on A_{inlet} / A_{drain} ratio for pitot tube at 60 $m \cdot s^{-1}$ for various drain hole areas

The gradual change of the dependence of *IAS / CAS* ratio on the A_{inlet} / A_{drain} ratio curve was found for all the drain hole combinations (see the curves in Figure 6). A small discrepancy between the curves was found and the independence of dimensions is not as significant as the independence of airspeed. A probable reason is described in the Discussion. Figure 7 shows the same information in the dynamic pressure form.

3. Discussion

3.1. Danger of gradual blockage of the pitot tube

The paper shows the gradual change of the IAS due to the gradual blockage of the pitot tube (see Figure 8). If the blocking ratio A_{inlet} / A_{drain} = 9 and the IAS is 99% of CAS, the airspeed error due to blockage is negligible. The IAS is 90% of CAS at blocking ratio A_{inlet} / A_{drain} = 1.6, the airspeed error must be taken into account. If the blocking ratio A_{inlet} / A_{drain} = 0.66, the IAS is 58% of CAS. For pilots, it is difficult to recognize the pitot tube blockage like in the Airbus A330 accident (Bureau d'enquêtes et d'analyses pour la sécurité de l'aviation civile, 2012). There are two possible gradual blocking scenarios presented in Table 6. If the drain hole is blocked before the inlet hole (first scenario), the speed will be almost equal to CAS until the entire pitot tube is blocked. The airspeed after blocking will be kept at the value before blocking. If the drain hole freezes later or does not freeze at all (the second scenario), the freezing of the inlet causes a decrease in IAS. The pilot's logical reaction is to increase CAS to keep the required IAS. This can lead to the maximum airspeed being exceeded. Therefore, the second situation can be even more critical than the first.

3.2. Influence of the number of drain holes

For different diameters and numbers of drain holes, a slight discrepancy of the measured gradual blocking curves was found. The reason is probably various throttling in various numbers of drain holes with different diameters (2 with a diameter of 0.5 mm and 2 with a diameter of 1 mm). The throttling in more holes is higher (the flow does not go through more holes with a total area equivalent to one hole

Table 6. Freezing of the pitot tube scenario

Scenario description	Level of freeze of the pitot tube	No freeze	Low freeze	High freeze	Total freeze	Change of speed to 288 $km \cdot h^{-1}$	Conclusion
	CAS ($m \cdot s^{-1}$)	60	60	60	60	80	
	CAS ($km \cdot h^{-1}$)	216	216	216	216	288	
The drain hole freezed out earlier than the inlet hole	IAS ($km \cdot h^{-1}$)	216	216	216	216	216	After change of the speed, pilot sees the IAS before both holes freezed out.
The inlet freezes out gradually, drain hole does not freeze at all	IAS ($km \cdot h^{-1}$)	216 [1)]	210 [2)]	150 [3)]	0	0	Pilot sees gradual decrease of the speed, which he probably starts to compensate with the increase of the airspeed up to exceeding the maximum speed.

Note: 1) $\frac{A_{inlet}}{A_{drain}} > 10$; 2) $\frac{A_{inlet}}{A_{drain}} = 3.6$; 3) $A_{inlet} / A_{drain} = 0.8$.

as easily as when it goes through one hole). Nevertheless, the measured deviation is still acceptable. For an accurate result, it is recommended to measure the gradual blocking curve for each pitot tube and type of blockage individually.

3.3. Potential of the described principle for gradual blockage detection

The gradual blocking curve IAS / CAS on A_{inlet} / A_{drain} is independent of velocity magnitude. In general, the detection of gradual blocking of the pitot tube can be very difficult even if we have more than one tube of the same parameters in the aircraft. The IAS error will increase similarly with gradual blockage. Therefore, it can be convenient to obtain the total pressure from two sources with different A_{inlet} / A_{drain} ratios. For clarification of the principle, assume that we have two pitot tubes. The first pitot tube with A_{inlet} / A_{drain} = 9, the second with A_{inlet} / A_{drain} = 2. If the first pitot tube inlet area decreases three times, you can see in Figure 8 that IAS will decrease to 97% of CAS. If the second pitot tube inlet area decreases three times, IAS will decrease to 58% of CAS according to the gradual blocking curve in Figure 5. The problem with the pitot tube blockage will be obvious for a pilot from the pressure difference. If the second pitot tube inlet is smaller, faster icing blockage is expected in this pitot tube. The different dynamic pressure (and IAS) on each pitot tube will be even higher. The information resulting from Figure 8 can be then used for the detection of gradual blockage of the pitot tube inlet. This will be the subject of further research for the design of a new system.

The gradual blockage of the pitot inlet should be possible to be detected even during an unaccelerated level flight. Therefore, the pilot will have time to get prepared for losing the IAS information. In a situation when the pilot knows that the airspeed indicator is not showing the correct information, he or she can use emergency procedures (Barthe, 2007). The detection of gradual blockage could prevent some aviation accidents that have occurred in the past due to the gradual blockage of the pitot tube (Bureau d'enquêtes et d'analyses pour la sécurité de l'aviation civile, 2012). This method of determination appears to be applicable without complex equipment.

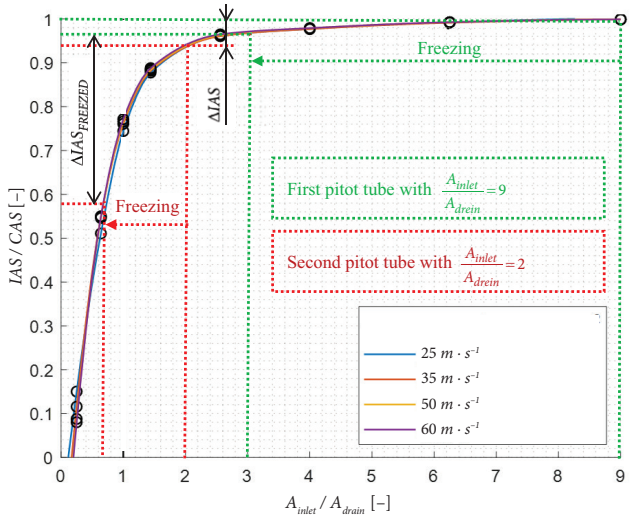

Figure 8. Gradual blocking curve *IAS / CAS* ratio A_{inlet} / A_{drain} ratio for a Pitot tube with 1 mm drain hole diameter

When using the principle presented in Figure 8, it would be necessary to use at least two pitot tubes with different parameters. For small aircraft, it is common to use only one tube. The new system should not complicate the speed measurement too much. This should be a priority when designing a new system. For large airliners, it is common to use two or more tubes, so the introduction to airliners should not be so complicated.

The system should be applicable to standard pitot tubes used on GA aircraft by adding a small ice detection tube with differential pressure sensors (on the wing or in the cabin and connected to extra pressure hoses). The results of this research do not provide proposals for a specific system for detecting gradual blockage of the pitot tube, but it describes possible principles for a future system.

Conclusions and future work

The paper has presented a study of the gradual blockage of total pressure inlet on pitot tube with drain holes. The leakage in drain holes results in a gradual decrease of IAS if the inlet diameter decreases. For describing the drain hole effect, gradual blocking curve was experimentally measured. The curve is independent of investigated velocity magnitude from 25 to 60 $m \cdot s^{-1}$. The curve slightly changes with a different number of drain holes. This is probably caused by various throttling and the Reynolds numbers in the drain holes. A new approach to the detection based on the drain hole effect has been presented, which is the key finding of this work. Using two pitot tubes with different A_{inlet} / A_{drain} ratios allows a detection of the gradual blocking before the full blockage by indicated airspeed difference. This finding is substantiated by experimental measurements in the wind tunnel test. In the future work, the detection system will be developed on the presented principle and tested in the practical condition. Using this principle in aircraft can help to detect the blocking of the pitot tubes.

Funding

This work was supported by the Specific research under Grant FSI-S-20-6288.

Disclosure statement

The authors would like to thank Assoc. prof. Jiří Hlinka, Dr. Pavel Zikmund, Ing. František Löffelmann, Mr. Joseph Smith, Mr. Vlastimil Jireš for their useful comments, which improved the quality of the work.

References

AAIB Bulletin 11/2020. (2020). *Serious incident*. https://assets.publishing.service.gov.uk/media/5f881884e90e07415e7f36c5/Airbus_A321-231_G-WUKJ_11-20.pdf

Australian Transport Safety Bureau. (2018). *Airspeed indication failure on také-off involving Airbus A330, 9M-MTK, Brisbane Airport, Queensland, on July 2018*. ATSB. https://www.atsb.gov.au/publications/investigation_reports/2018/aair/ao-2018-053

Ayra, E. S., Sanz, Á. R., Valdés, R. A., Comendador, F. G., & Cano, J. (2020). Detection and warning of ice crystals clogging pitot probes from total air temperature anomalies. *Aerospace Science and Technology*, *112*, 105874. https://doi.org/10.1016/j.ast.2020.105874

Barthe, J. (2007). Unreliable speed. *Safety First, 2007*(05), 7.

Bureau d'enquêtes et d'analyses pour la sécurité de l'aviation civile. (2012). *Final Report: Airbus A330-203*. https://reports.aviation-safety.net/2009/20090601-0_A332_F-GZCP.pdf

European Aviation Safety Agency. (2013). *Stall and spin loss of control*. https://havarikommissionen.dk/media/9238/ga8.pdf

Federal Aviation Administration. (2016). *Pilot's handbook of aeronautical knowledge*. https://www.faa.gov/regulations_policies/handbooks_manuals/aviation/phak

Freeman, P., Seiler, P., & Balas, G. J. (2011). Robust fault detection for commercial transport air data probes. *IFAC Proceedings Volumes, 44*(1), 13723–13728. https://doi.org/10.3182/20110828-6-IT-1002.03750

Flight Safety Foundation. (1995). Rejected takeoff in icy conditions results in runway overrun. *Accident Prevention*, *52*(5). https://flightsafety.org/ap/ap_may95.pdf

Genito, N., Corraro, F., Garbarino, L., Vitale, A., De Lellis, E., Bibby, D., & Jones, K. G. (2018). *U.S. Patent No. 9,983,023*. Patent and Trademark Office. https://patentimages.storage.googleapis.com/ed/8d/67/4fcbf0a43452a7/US9983023.pdf

Guo, D., Wang, Y., Zhong, M., & Zhao, Y. (2018). Fault detection and isolation for Unmanned Aerial Vehicle sensors by using extended PMI filter. *IFAC-PapersOnLine, 51*(24), 818–823. https://doi.org/10.1016/j.ifacol.2018.09.669

Hansen, S., Blanke, M., & Adrian, J. (2010). Diagnosis of UAV pitot tube defects using statistical change detection. *IFAC Proceedings Volumes, 43*(16), 485–490. https://doi.org/10.3182/20100906-3-IT-2019.00084

Jäckel, R., Tapia, F., Gutiérrez-Urueta, G., & Jiménez, C. M. (2020). Design of an aeronautic pitot probe with a redundant heating system incorporating phase change materials. *Flow Measurement and Instrumentation, 76*, 101817. https://doi.org/10.1016/j.flowmeasinst.2020.101817

Jackson, D. A. (2015). Concept of a Pitot tube able to detect blockage by ice, volcanic ash, sand and insects, and to clear the tube. *Photonic Sensors, 5*(4), 298–303. https://doi.org/10.1007/s13320-015-0272-x

Jarvinen, P. O. (2011). *U.S. Patent No. 8,060,334*. U.S. Patent and Trademark Office.

Japan Transport Safety Board. (2018). *Aircraft serious incident investigation report*. JTSB. https://www.mlit.go.jp/jtsb/eng-air_report/JA04JJ.pdf

Lv, X., Guan, J., Wang, S., Zhang, H., Xue, S., Tang, Q., & He, Y. (2020). Pitot tube-based icing detection: Effect of ice blocking on pressure. *International Journal of Aerospace Engineering*, *2020*, 1902053. https://doi.org/10.1155/2020/1902053

Nathan, V. T., & Anandappan, T. (2014). *U.S. Patent No. 8,914,164*. U.S. Patent and Trademark Office.

National Transportation Safety Board (NSTB). (2013). *NTSB Identification: ERA12FA115*. https://www.ntsb.gov/_layouts/ntsb.aviation/brief.aspx?ev_id=20111220X20005&key=1

Oxford Aviation Academy. (2008). *Aircraft General Knowledge, 4*. United Kingdom.

Parker, Ch. L. (2007). *12 Steps to safe takeoffs*. AOPA. https://www.aopa.org/news-and-media/all-news/2007/june/flight-training-magazine/12-steps-to-safe-takeoffs

Sun, K., & Gebre-Egziabher, D. (2020, April). A fault detection and isolation design for a dual pitot tube air data system. In *2020 IEEE/ION Position, Location and Navigation Symposium (PLANS)* (pp. 62–72). IEEE. https://doi.org/10.1109/PLANS46316.2020.9110179

The Interstate Aviation Committee. (2018). *Accident investigation Antonov An-148-100B*. https://mak-iac.org/en/rassledovaniya/an-148-100b-ra-61704-11-02-2018/

Notations

A_{drain} – Pitot drain hole area;
A_{inlet} – Pitot inlet hole area;
AoA – Angle of attack;
CAS – Calibrated airspeed;
D_{drain} – Pitot drain hole diameter;
D_{inlet} – Pitot inlet hole diameter;
GPS – Global Position System;
IAC – International aviation committee;

IAS – Indicated airspeed;
IMU – Inertial Measurement Unit;
ISA – International Standard Atmosphere;
k_A – Larger to lower hole area parameter;
MFD – Multifunction Flight Display;
PFD – Primary Flight Display;
p_D – Dynamic pressure;
p_S – Static pressure;
p_T – Total pressure;
TAS – True airspeed;
UAS – Unmanned Aerial System;
UAV – Unmanned Aerial Vehicle;
V – Airspeed;
ρ_0 – Air density at 0 m ISA.